Ilomuanya et al. Beni-Suef University Journal of Basic and Applied Sciences (2020) 9:31
https://doi.org/10.1186/s43088-020-00057-9

Beni-Suef University Journal of Basic and Applied Sciences

RESEARCH Open Access

Polylactic acid-based electrospun fiber and hyaluronic acid-valsartan hydrogel scaffold for chronic wound healing

Margaret O. Ilomuanya[1,2*], Prosper S. Okafor[1], Joyce N. Amajuoyi[1], John C. Onyejekwe[1], Omotunde O. Okubanjo[1], Samson O. Adeosun[3] and Boladale O. Silva[1]

Abstract

Background: In this study, the chronic wound healing ability of PLA-based electrospun nanofibers loaded with hyaluronic acid, valsartan, and ascorbic acid is explored. PLA-based scaffolds were fabricated by electrospinning, followed by loading the scaffolds with different concentrations of hyaluronic acid, valsartan, and ascorbic acid hydrogels. The produced formulations were characterized by scanning electron microscopy imaging (SEM), tensile strength testing, Fourier-transform infrared spectroscopy (FTIR), and differential scanning calorimetry (DSC). An in vitro drug release study was conducted to monitor the release of valsartan from the different formulations. This was followed by exploring the wound healing effects of the scaffolds in alloxan-induced diabetic rats and comparing the wound healing effects with positive and negative controls.

Results: The average diameter of the fibers was in the range of 300 to 490 nm with high porosity in the range of 63.90 to 79.44%, offering a large surface area-to-volume ratio, enhanced drug solubility, oxygen permeability, and fluid uptake. The presence of valsartan significantly impacted on the re-epithelization rate. Percentage re-epithelization rate was 31.2% ± 1.77% in the absence of treatment. Histologic section of tissue showed skin with underlying loose fibro-collagenous stroma (dermis) containing sebaceous glands and hair follicles for animals treated with VA, VB, VC, and VD. All the scaffolds reduced the number of inflammatory cell infiltrates at the wound site compared to the no treatment and conventionally treated groups. Conventional antibiotic treatment and VD (electrospun biomimetic scaffolds containing ascorbic acid) had % re-epithelization rates of 59.45% ± 1.69% and 62.01% ± 1.68% which were significantly lower than the PLA/HA-valsartan hydrogel scaffolds with VB having the highest % re-epithelization rate of 85.5% ± 1.7% (Figure 4B & 5C).

Conclusion: This study explored the use of biomimetic polylactic acid-based electrospun fiber and HA-valsartan hydrogel scaffold incorporating topical angiotensin receptor blockers to successfully accelerate wound healing. The novel PLA-based electrospun fibers loaded with hyaluronic acid-valsartan hydrogels were stable and possessed proven diabetic wound healing property. This was as a result of the known biomimetic effect of the fibers and increased re-epithelization facilitated by the hydrogels containing valsartan.

Keywords: Electrospun fibers, Valsartan, Hydrogels, Wound healing, Polylactic acid

* Correspondence: milomuanya@unilag.edu.ng; milomuanya@popcouncil.org
[1]Department of Pharmaceutics and Pharmaceutical Technology, Faculty of Pharmacy, University of Lagos, PMB 12003, Surulere, Lagos, Nigeria
[2]Center for Biomedical Research, Population Council, 1200 York Avenue, New York 10065, USA
Full list of author information is available at the end of the article

1 Background

Chronic non-healing wounds are wounds that have failed to progress through a timely sequence of repair or that proceeds through the wound healing process without restoring anatomic and functional results [1, 2]. A physiologic impairment is usually responsible for slowing or preventing the wound healing process. Chronic wounds include but are not limited to pressure ulcers, diabetic foot ulcers, venous ulcers, and arterial insufficiency ulcers. Chronic wounds share similar characteristics which include high level of proteases, elevated inflammatory markers, low growth factor activity, and reduced cellular proliferation [3]. The presence of metabolic conditions in the patients as well as infections also result in chronic wounds. Antibiotic-based dressings, like neomycin, silver, and iodine, have been developed to avoid infections in wounds, which have been noted as one of the main causes of delayed wound healing. However, there is a risk of allergy and microbial resistance in the use of these antibiotic-based dressings [1]. Advances in wound management have also led to the development of active dressings that facilitate the wound healing process as well as techniques such as vacuum-assisted closure to remove cytokines and proteases [2]. Problems with the cost of wound healing therapies, wound reoccurrences, poor absorption, and the difficulties in healing chronic wounds have presented serious obstacles in the management of chronic wounds. Electrospinning is an effective technique used to fabricate a nanofiber similar to the natural ECM by simply supplying an electric field to a polymer. In addition, electrospun matrices have a large specific surface area-to-volume ratio, high porosity, and ease of control over the diameter, composition, and morphology of the constituent fibers [3–5]. Electrospun materials containing natural polymers like hyaluronic acid have been used as wound dressing materials. In addition, electrospun scaffolds can be incorporated with dermal and epidermal cell lines, and it has been reported that collagen and PCL (poly (ε-caprolactone) electrospun scaffolds with dermal fibroblast promoted better wound healing than acellular scaffolds [3]. Electrospun scaffolds have also been used for controlled release of drugs [4], herbal extracts [5], and growth factors like EGF (epidermal growth factor) [5] which have shown successful improvements in chronic wound healing. Studies have also shown the effective use of valsartan topical formulations in animal models in the treatment of chronic diabetic wounds by aiding angiogenesis, increased fibroblast proliferation, re-epithelization, reduced oxidative stress, and increased blood flow to the site of injury [6].

Excellent wound dressings maintain a warm and moist environment that accelerates wound healing [7]; however, traditional dressings such as gauze and cotton wool are neither able to maintain an optimal moist wound environment nor have biological activity on the wound healing process. Thus, the modern concept of moist wound dressings is employed to design the wound care products [8–11], and hydrogels have shown promise as wound dressing materials as they are able to create a hydrated environment to help promote the body's wound healing response [12]. A previous study showed that the *Astragalus polysaccharide*-loaded poly(lactic-co-glycolic acid) (PLGA) fibrous mats accelerate diabetic wound healing by enhancing the restoration of skin microcirculation [10, 11].

Polymers like polyvinyl alcohol (PVA) and hyaluronic acid are commonly used in the fabrication of hydrogels for wound healing [13]. Studies have shown that hydrogels composed of hyaluronic acid and chitosan have been used to deliver the angiogenic promoting growth factor, possess antibacterial property, and promote blood clotting [14]. Utilization of animal models becomes critical in measuring histomorphometric parameters of healing which would justify utilization of hyaluronic acid and valsartan in the proposed formulation. Cell-line based studies are limited in this regard. The aim of the study is to develop and characterize a biomimetic PLA-based electrospun fibers loaded with HA-valsartan hydrogels for chronic wound healing evaluation in an animal model.

2 Method

2.1 Materials

The materials are as follows: polylactic acid (PLA 250, 000 g/mol is ~ 20 wt %) (Merck KGaA, Darmstadt, Germany), dichloromethane (Merck KGaA, Darmstadt, Germany), glutaraldehyde (Merck KGaA, Darmstadt, Germany), valsartan (Analytical Standard N-(1-Oxopentyl)-N-[2′-(2H-tetrazol-5-yl)[1,1′-biphenyl]-4-yl]methyl]-L-valine, Sigma-Aldrich, St. Louis, USA), Valsartan Pharmaceutical Grade (CAS Number 137862-53-4 Shanghai Macklin Biochemical Co. Ltd, China) and 99% absolute ethanol (Sigma-Aldrich, St. Louis, USA), ascorbic acid (Merck KGaA, Darmstadt, Germany), sodium metabisulphite, alloxan monohydrate (Sigma-Aldrich, St. Louis, USA), hyaluronic acid (HA), sodium salt powder (Sigma-Aldrich St. Louis, USA), and phosphate-buffered saline (Quality Biological, USA). The water used in the experiment was Milli-Q water (Millipore, USA). All other chemical reagents were of analytical grade and were used without further purification.

2.2 Electrospun scaffolds design and fabrication

Twenty percent w/v of the PLA polymer was dissolved in 100 mL dichloromethane; 0.2% v/v of glutaraldehyde was introduced into the solution with stirring at 150 rpm at 25 °C for 4 h, until complete dissolution of the polymer was obtained [15]. Electro-spinning of the

prepared solution was carried using 20 mL plastic syringes equipped with 21 G gauge needles. The loaded syringe was placed in a syringe pump and operated at a flow rate of 0.1 mL/min. The solution was then electrospun at a voltage of 25 kV onto a static collector wrapped with aluminum foil paper. A polyethylene capillary tube was used to connect the syringe and the needle which was set up vertically to the collector. The collector was a rectangular copper plate covered with aluminum foil and located 37 cm from the needle tip for the deposition of scaffolds [15].

2.3 Formulation of HA-valsartan hydrogel scaffold

The HA-valsartan hydrogel was prepared as described in previous literature [6, 16]. Hyaluronic acid (HA) sodium salt powder (1 g) was dissolved in 100 mL double-distilled water. 2.7% w/v sodium periodate solution and 0.2% w/v sodium metabisulfite was gradually introduced into the hydrogel mix in a 0.5:0.5:1 ratio, and the mixture was left to oxidize for 24 h after which it was dialyzed. The varying concentrations of ascorbic acid and valsartan added to the hydrogel mixture as shown in Table 1. The formulated hydrogel was then dissolved overnight in phosphate-buffered saline (pH 7.4) to 6% (w/v). This formulated hydrogel was then loaded on the surface of the electrospun PLA scaffold (in a weight ratio of 4:1) and allowed to dry in a desiccator at 25 °C ± 0.5 °C.

2.4 Morphological and chemical characterization

2.4.1 Scanning electron microscopy

The surface morphology of the fabricated nanofibrous scaffolds was determined via field emission scanning electron microscopy (FEG-SEM) using a Phenom World Eindhoven Phenom ProX scanning electron microscope. The scaffolds were cut into small pieces of 5 mm × 5 mm. Before observation, each sample was coated using a gold sputter coater for 2 min. The 5 mm × 5 mm cut samples were then mounted over the studs using a carbon tape and analyzed at 15 kV. All samples were analyzed in triplicates [15].

2.4.2 Fourier-transform infrared spectroscopy (FTIR)

The chemical structure or presence of functional groups present in the scaffolds was confirmed by FTIR using an Agilent Technologies Cary 630 spectrophotometer. The spectra were recorded in the range of wave numbers from 4000 to 500 cm^{-1} to characterize the absorption bands of the nanofibers of PLA. Samples of nanofibrous scaffolds were dehydrated by vacuum drying by vacuum drying at 45 °C and later placed over the diamond crystal for the FTIR analysis. Twenty scans were recorded for each spectrum. Smoothing was done where necessary to reduce the noise without loss of any peak [17].

2.4.3 Differential scanning calorimetry

Analysis of any possible polymer interaction and the thermal transitions was recorded using differential canning calorimetry via Mettler Toledo® Differential Scanning Calorimeter DSC-2/700/214 at 37 °C to 450 °C. Five milligrams of the scaffolds was taken into aluminum pans and was then hermetically sealed. A controlled heating and cooling rate was maintained at 10 °C/min in nitrogen atmosphere [17].

2.5 Mechanical characterization

2.5.1 Measurement of the mechanical strength of the hydrogel-loaded electrospun scaffolds

The tensile or mechanical strength of the nanofibrous scaffolds were measured using a universal testing machine. The cross-linked scaffolds were cut into tapered "dog bone" sections of dimensions 50 mm × 10 mm and tested at an ambient temperature of 25 °C ± 0.5 °C and humidity of 60%. The resulting scaffolds were then mounted between two clamps and stretched at a rate of 50 mm/min with an applied load range of about 50 N and gauge length of 50 mm [18]. The tensile strength was recorded in triplicate.

The pH, viscosity, and gel index of the hydrogel formulations were determined at 25 °C ± 0.5 °C. The viscosity was determined at 20–60 rpm using spindle 4 of a cone and plate viscometer (DV-E Digital viscometer, Brookfield Engineering Laboratories Middleboro, MA, USA) at 25 °C ± 0.5 °C. This was evaluated exponentially using the power law according to Eq. 1.

$$T = K\,Dn \tag{1}$$

where T is shear stress, K is gel index (GI), D is shear rate, and n is flow index.

Table 1 Composition of polylactic acid-based electrospun fiber and HA-valsartan hydrogel scaffold

Formulation	Hydrogel component				Electrospun component
	Hyaluronic acid (%w/v)	Valsartan (%w/v)	Ascorbic acid (%w/v)	Sodium metabisulfite (%w/v)	
VA	0.1	1.5	0.5	0.2	20% w/v PLA cross-linked using 0.2% v/v glutaraldehyde
VB	0.2	1.0	0.75	0.2	
VC	0.3	1.5	0.5	0.2	
VD	0.4	–	0.75	0.2	

2.5.2 In vitro release study

The release of valsartan from the PLA/HA-valsartan hydrogel scaffold was measured using UV spectroscopy by placing 2.5 × 2.5 cm^2 of scaffolds in 20 mL of release medium, phosphate-buffered saline (PBS), at a pH of 7.4. The temperature was maintained at 37 °C ± 0.5 °C and stirring of the system at 50 rpm. One milliliter of aliquot sample was withdrawn, at fixed time intervals, and the same amount of fresh solution was added back to the release medium to maintain sink conditions. The samples were analyzed using an UV spectrophotometer at 250 nm.

2.6 In vivo wound healing

2.6.1 Determination of skin irritancy via patch test

0.5 g of polylactic acid-based electrospun fiber and HA-valsartan hydrogel scaffolds were applied to the shaved dorsal surface (3 cm^2) of male Wistar rats (n = 3/treatment). The skin was visually examined for erythema and edema 1 h after application to check for skin irritation.

2.6.2 In vivo wound healing study

Forty male healthy treatment naïve rats aged 12 weeks old weighing 140–150 g and purchased from Joss Rattery® breeds Ibadan Oyo State Nigeria were used in this study. They were allowed to acclimatize in their new environment for 7 days before the start of the study. The animals were maintained under controlled temperature (28 ± 2 °C), relative humidity (45 ± 10%), and a 12 h light and dark cycle; lights went off at 7 pm. They had access to a standard 2016 diet, i.e., Harlan Teklad Diet (Harlan Teklad Bircester U.K.) and clean drinking water ad libitum. The animals were kept in 600× 390 × 200 mm polycarbonate cages housed in well-aerated rooms with a 12 h light/12 h dark cycle at 28 °C ± 2 °C and fed with standard rodent diet and water ad libitum. This study followed the National Institutes of Health guide for the care and use of laboratory animals (NIH Publication No. 8023, revised in 1978) [19]. All the experiments abided by the institutional guidelines approved by author's institutions' Health Research Ethical Committee CMUL/HREC/07/19/564. As shown in the experimental timelines in Fig. 1, diabetes was induced using the method of Mendes et al. [20], by giving two intra-peritoneal injections of alloxan monohydrate (150 mg/kg body weight) at 48-h intervals in rats fasted overnight. Alloxan causes an insulin-dependent diabetes mellitus also called "alloxan diabetes," in these animals, with characteristics like type 1 diabetes in humans [20]. The blood sample was obtained by tail clipping method, and glucose levels were checked using pre-calibrated Accu-Chek Active® glucometer.

The average random blood glucose level of normal rats was found to be 136 mg/dL whereas the fasting blood glucose level (after overnight fasting) was 92.7 mg/dL. However, 48 h after alloxan administration, the fasting blood glucose level was found to be 187.3 mg/dL, whereas the random blood glucose levels were 442.3 mg/dL. Such animals were considered severely diabetic and selected for wound healing studies [20].

Diabetic rats were taken and distributed in six different groups with each group containing four diabetic rats (n = 4). The distribution of the diabetic rats was done via simple randomization. All the diabetic rats in all experimental groups were exposed to the same environmental conditions. Thee rats had a mean body weight of 147.43 ± 3.2 g at the start of the experiment. The rats were anesthetized by giving 0.1 mL of ketamine-xylazine (50 mg ketamine/ kg body weight and −5 mg xylazine/ kg body weight) intraperitoneally. Hair was removed by using hair removing cream; disinfection was carried out which precluded the creation of full-thickness wounds extending through the *panniculus carnosus* using a punch biopsy instrument (diameter 5 mm, accu® punch) after which the various dressing materials were applied. Ibuprofen suspension was administered to all the animals to control pain [20]. Treatment commenced 24 h after the wound was created; all formulations (4 cm × 4 cm scaffolds) including the controls were fixed on the surface of the wounds. At predetermined intervals, the wound size was examined using a digital camera with image calibration capacity. Treatment was performed daily by the same person at the same time. The relative wound size reduction at treatment time t in days was calculated according to Eq. 2; Ao is the wound diameter (mm) at time t = 0 and At is the wound diameter at time t.

$$\text{Relative wound size reduction } (\%) = [\text{Ao}-\text{At}/\text{Ao}] \times 100 \quad (2)$$

2.6.3 Histological test

After the 14-day wound healing examination period, the rats were humanely euthanized, and the wounded area was sampled by trimming to include the dermis and hypodermis. The trimmed skin layers were fixed in 10%

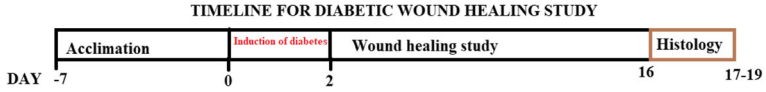

Fig. 1 Experimental timelines

neutral buffered formalin. After paraffin embedding, 3–4 μm sections were prepared. Representative sections were then stained with hematoxylin and eosin (H&E). The light microscopic examination for histological profiles of individual rat skin sections was then performed [15].

2.6.4 Histomorphometry

Using a digital image analyzer (DMI-300, DMI, South Korea), the histological skin samples were evaluated for the numbers of micro vessels in granulation tissues (vessels/mm^2 of field), percentages of collagen-occupied regions in granulation tissues (%/mm^2 of field), the desquamated epithelium regions (mm), numbers of infiltrated inflammatory cells in granulation tissues (cells/mm^2 of field), and thicknesses of central regions of granulation tissues (mm from epidermis to dermis). Re-epithelization was calculated as in Eq. 3.

$$\text{Re–epithelization}\ (\%) = \frac{\text{Total wound length (mm)} - \text{Desquamated epithelium region (mm)} \times 100}{\text{Total wound length (mm)}} \quad (3)$$

2.7 Statistical analysis

The data was presented as mean ± standard deviation of more than three experimental values for every variable and analyzed by one-way ANOVA followed by Dunnett's test using GraphPad Prism version 5. *P* value of less than 0.05 was considered statistically significant.

3 Results

3.1 Morphological and chemical characterization

The HA-valsartan hydrogel exhibited pH between 5.67 and 5.83, which put the hydrogels in the acidic range hence its suitability for chronic wound care. The gel index was above 1 hence its ability to be easily loaded unto the electrospun PLA scaffold. Both the hydrogel and the PLA/HA-valsartan hydrogel scaffold showed no skin irritancy when applied (Table 2). The skin irritancy test showed that both the HA-valsartan hydrogels as well as the PLA/HA-valsartan hydrogel scaffold was tolerable to the skin. There were no signs of erythema and edema observed.

3.2 Scanning electron microscopy

The scanning electron microscopy (SEM) results of the hydrogel-loaded nanofibers gave a clear view of the fibers with variation in fiber morphology due to respective PLA/HA-valsartan hydrogel scaffold constitution. The SEM images showed non-uniform ribbon-like nanofibrous membranes embedded with pores were fabricated (Fig. 2). There was an indicative absence of beading in the fibers, showing that the electrospinning parameters were well optimized. The smooth surface of the fibers seen in Fig. 2 VA, VB, VC, and VD will ensure that there is no risk of the dressing adhering to the wound surface as seen with traditional cotton gauze dressings. This is especially critical in excess wound drainage, where wound re-dressing can cause tissue injury thus slowing down the wound healing process [21].

The deposition of the hydrogels loaded on the fibers can be clearly seen as a dense white opacity within the fibers (Fig. 2 SEM photographs of formulations VA, VB, VC, and VD). However, this dense white opacity was not pronounced in VA due to its lower concentration of hyaluronic acid and ascorbic acid. The scaffolds, though fabricated using the same concentration of polylactic acid (20% w/v), exhibited clear differences in the average diameter and porosity due to the presence of other additives which varied across VA, VB, VC and VD (Table 1). The average diameters of scaffolds VA, VB, VC, and VD were 490 ± 54 nm, 300 ± 56 nm, 360 ± 78 nm, and 370 ± 98 nm respectively (Fig. 2e). VA had the highest average diameter. The average porosity of the scaffold VA, VB, VC, and VD were 76.73 ± 0.95%, 79.43 ± 1.18%, 63.90 ± 1.07, and 65.76 ± 1.42% respectively. Scaffolds VC and VD exhibited the lower average porosity than VA and VB. Hyaluronic acid concentration influenced scaffold porosity, with higher concentration of HA producing scaffolds with lower average porosity.

Table 2 Physicochemical characterization of PLA/HA-valsartan hydrogel scaffolds

PLA/HA-valsartan hydrogel scaffold	HA-valsartan hydrogel characterization				PLA/HA-valsartan hydrogel scaffold characterization					
	pH	Viscosity (MPa)	Gel index	Skin irritancy	Skin irritancy	% drug content	Kinetic model elaboration of valsartan release from scaffolds			
							Zero order (K_0)	First order (K_f)	Higuchi (K_H)	Korsmeyer-Peppas (K_k)
VA	5.67 ± 0.09	1200 ± 1.1	1.12	Nil	Nil	91.92 ± 0.76	0.964	0.812	0.996	0.976
VB	5.66 ± 0.1	1099 ± 0.9	1.24	Nil	Nil	90.37 ± 1.16	0.980	0.904	0.998	0.998
VC	5.68 ± 0.1	1150 ± 0.5	1.33	Nil	Nil	90.55 ± 1.09	0.970	0.874	0.997	0.995
VD	5.83 ± 0.08	1210 ± 0.6	1.45	Nil	Nil	–	–	–	–	–

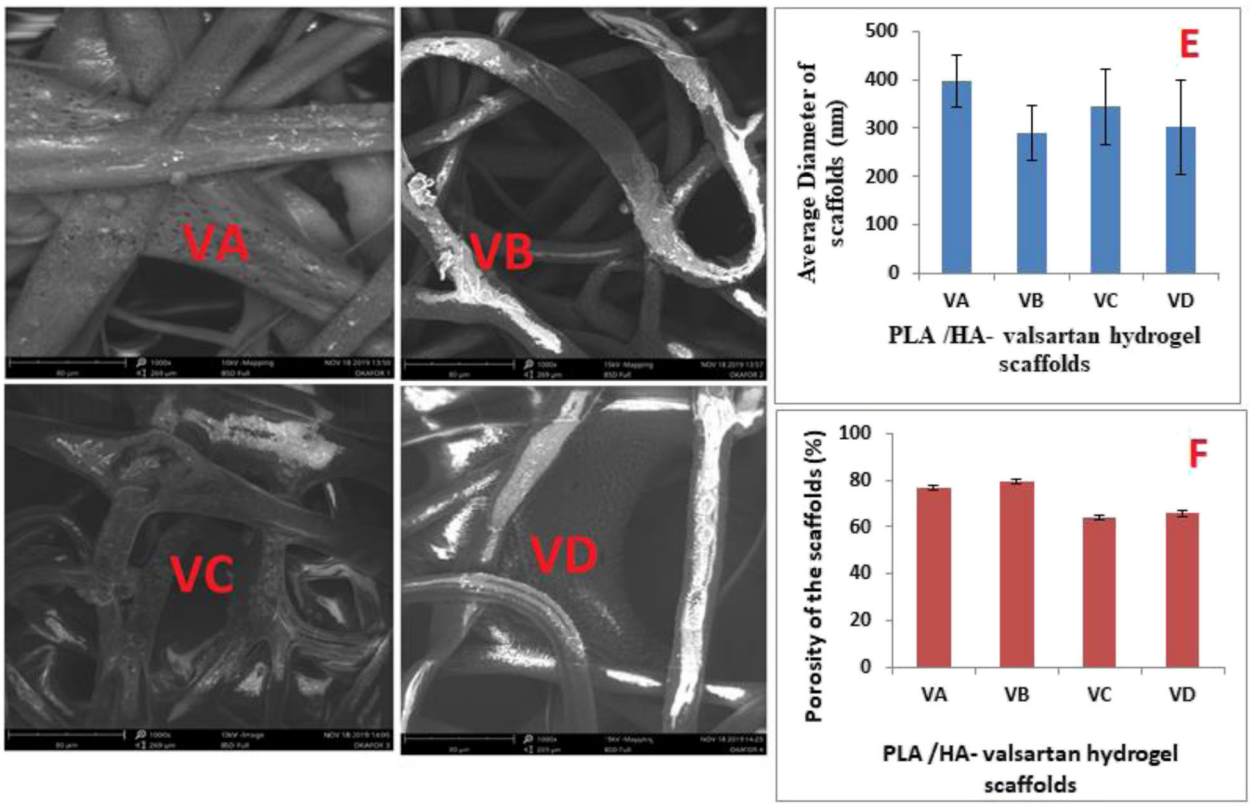

Fig. 2 Scanning electron microscopy of the PLA/HA-valsartan hydrogel scaffold VA, VB, VC, and VD. **E** Average diameter of the scaffolds. **F** Percentage porosity of the scaffolds

3.3 Fourier-transform infrared spectroscopy (FTIR) and differential scanning calorimetry (DSC) of the PLA/HA-valsartan hydrogel scaffold

3.3.1 Fourier-transform infrared spectroscopy (FTIR)

Figure 3a shows the FTIR spectra in the region 4000–500 cm^{-1} of the hydrogel scaffolds. From the FTIR spectra of VA, the peaks at 2948 and 2870 cm^{-1} are attributed to C–H stretching from the –CH2 group. The absorption bands at 1454 and 1383 cm^{-1} originated from C–H stretching from the –CH3 group. The absorptions at 1454 cm^{-1} are attributed to C–H deformation from –CH2. The bands at 1182, 1129, and 1081 cm^{-1} originated from C–O–C bending vibrations. The bands at 865 and 757 cm^{-1} are due to C–C stretching vibrations. The absorption bands of pure valsartan indicating N–H stretching were seen to shift to higher wave numbers of 3432, 3448, and 3444 cm^{-1} in VA, VB, and VC, respectively.

The recorded characteristic absorption peaks the C=O stretching vibration at 1750 cm^{-1} for neat PLA [22] is seen to slightly shift in all hydrogel scaffolds. This absorption peak is seen to shift to 1751 cm^{-1}, and this peak position shifted slightly to lower wave numbers of 1744, 1744, and 1748 cm^{-1} in VB, VC, and VD, respectively, where the samples contained higher concentrations of hyaluronic acid and ascorbic acid in the hydrogels. This suggests some interaction between the PLA and the compounds in the hydrogels exists.

3.3.2 Differential scanning calorimetry (DSC)

The DSC graph of heat flow (mW) versus temperature (°C) for the hydrogel-loaded fibers is shown in Fig. 3b. The spectra showed four features typical of semi-crystalline thermoplastics like heat flux at glass transition temperature (Tg), crystallinity, a melting endotherm, and decomposition. The Tg of VA, VB, VC, and VD at 70.02, 74.05, and 71.60 °C, respectively, is slightly higher than that of normal recorded values for PLA (50–60 °C) [22], while the Tg of VC at 60.19 °C was within expected values, indicating a correlation between glass transition temperature and the hydrogel loading. The decomposition temperatures of VA, VB, VC, and VD were recorded at 319.56, 325.36, 329.18, and 285.45 °C, respectively.

3.4 Mechanical characterization

3.4.1 Measurement of the mechanical strength of the hydrogel-loaded electrospun scaffolds

The mechanical properties of nanofibers are dependent on factors like the polymer used, fiber orientation, fiber length, fiber surface morphology, and the cohesion

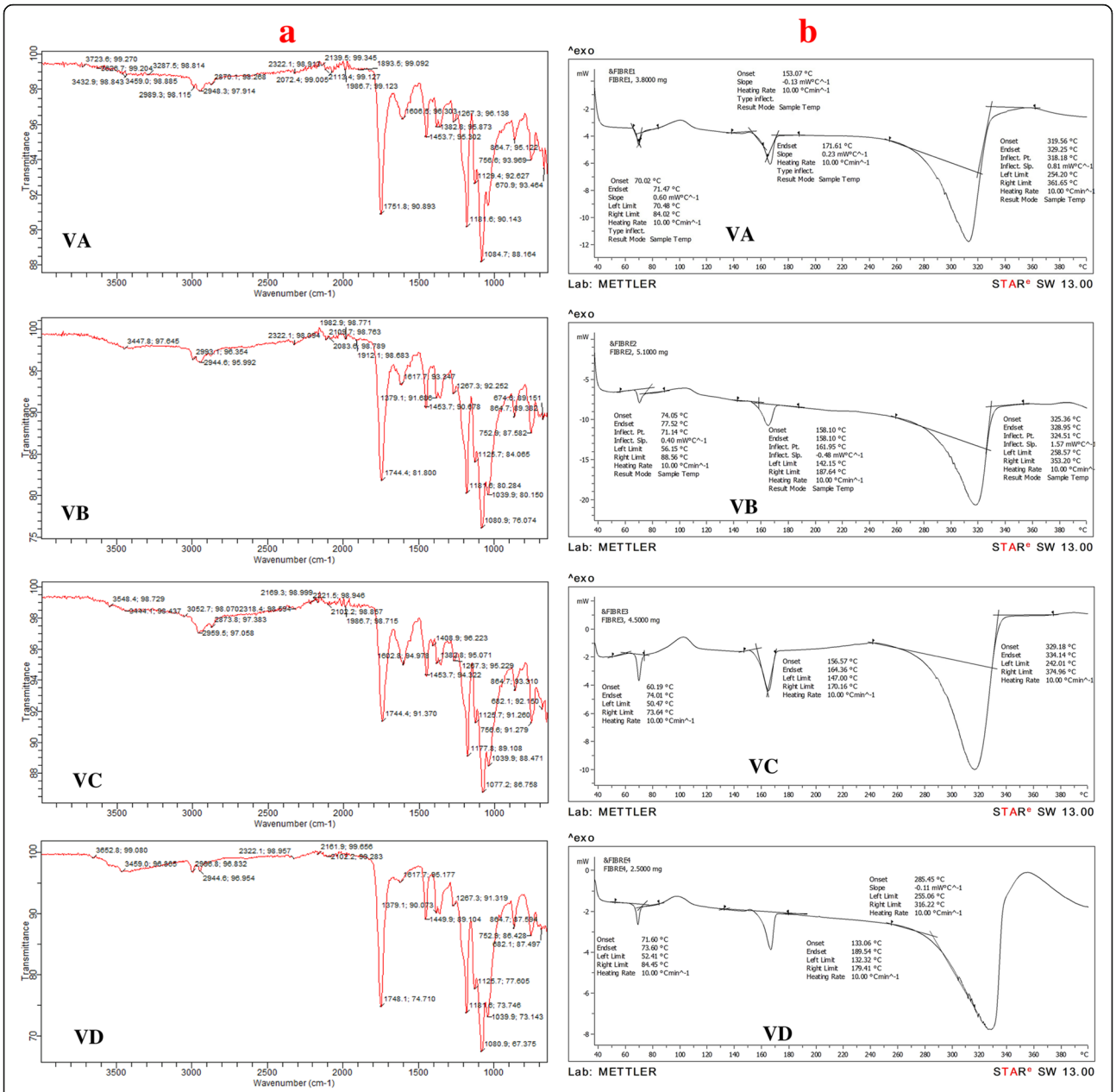

Fig. 3 (a)FTIR spectra of PLA/HA-valsartan hydrogel scaffolds VA, VB, VC, and VD. (b) DSC scans of PLA/HA-valsartan hydrogel scaffolds VA, VB, VC, and VD

frictional forces between the fibers. The tensile strength and elastic modulus graphs for the hydrogel-loaded scaffolds (Fig. 4a, b) showed that the scaffolds possessed adequate strength for utilization as a wound dressing material. VA, VB, VC, and VD scaffolds exhibited tensile strength of 0.92 ± 0.007, 1.12 ± 0.04, 1.12 ± 0.21, and 0.63 ± 0.12 MPa, respectively, and elastic modulus of 47.99 ± 3.76, 48 ± 1.72, 55.33 ± 13.8, and 46.91 ± 8.59 MPa respectively. This is consistent with literature for desired tensile strengths of wound dressing materials obtained via electrospinning [3, 22].

3.4.2 In vitro release study

The in vitro drug release profile was evaluated using different correlation coefficient (r^2) of varying mathematical models. The mathematical model with the highest degree of correlation coefficient r^2 determined the mechanism of drug release [23]. Higuchi square root model showed highest r^2 value compared to other models (0.998, 0.998, and 0.998 for VA, VB, and VC respectively as shown in Table 1). The release of valsartan from the scaffold involved the simultaneous penetration of surrounding liquid and dissolution and leaching out

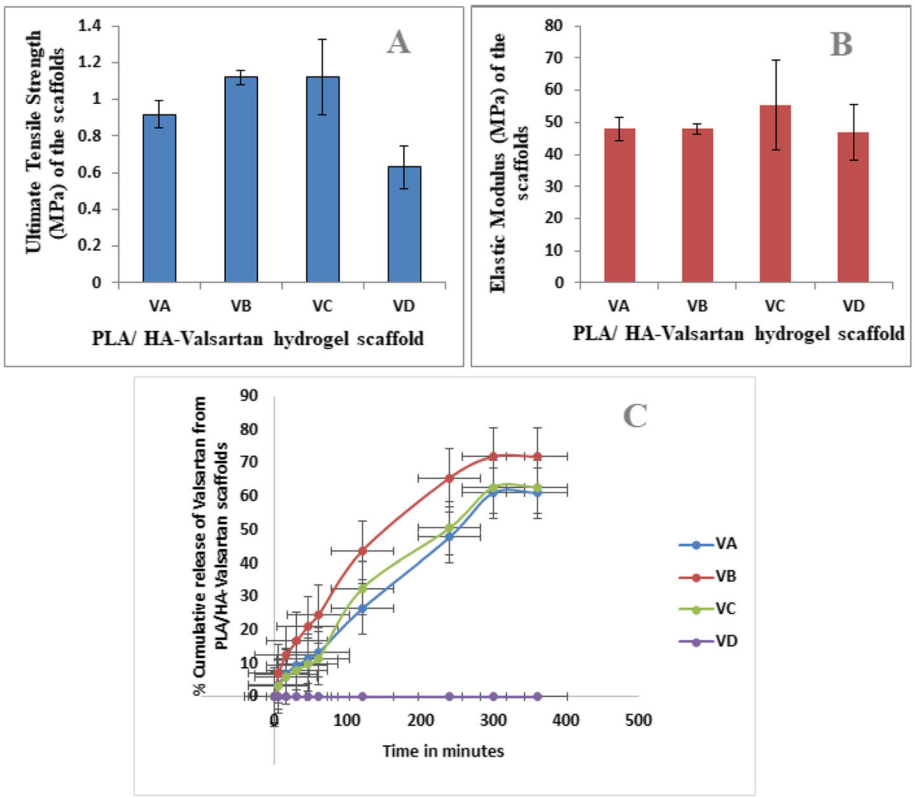

Fig. 4 **a** Ultimate tensile strength. **b** Elastic modulus. **c** Cumulative release of valsartan from PLA/HA-valsartan scaffolds VA, VB, VC, and VC

of valsartan, through channels or pores on the hydrogel scaffolds due to the high porosity of the formulation. The Korsmeyer-Peppas slope exponent (n) was between 1.94 and 2.0, which confirmed that valsartan release was characterized by super case II transport where an increase in valsartan release was observed with a higher drug diffusion coefficient [23].

The PLA/HA-valsartan scaffolds exhibited desired drug content after the hydrogel was loaded on the electrospun fiber (Table 1). The SEM showed even distribution of the hydrogels within the fibers hence facilitating a graded release of valsartan during the in vitro release study. There was a cumulative valsartan release of 11.56 ± 0.76 to 24.67 ± 0.46% from the samples in 60 min. This could be as a result of the interaction or binding of the compounds in the hydrogels to the nanofibers, as confirmed in the FTIR result. At 120 min, VB showed the highest amount of drug release with a cumulative release of 43.75% compared to VA and VC with 26.45% and 32.56% respectively (Fig. 4c). Cumulative release of over 70% of valsartan from the scaffolds occurred at 350 min with VB. This singular result significantly shows that the sustained release of valsartan occurred over a period of 6 h, and permanent entrapment of valsartan did not occur within the electrospun scaffold.

3.4.3 In vivo wound healing study and histopathology

The macroscopic presence of wounds treated with sterile gauze, hydrogel-loaded nanofiber wound dressing, and non-treated wounds on several post-operative days are illustrated in Fig. 5a. Each wound was studied for a time period of 14 days post-operation. There was no indication of necrosis, except for the non-treated wounds. At the onset of the experiment when the injury was inflicted, there was an outpouring of lymphatic fluid and blood. Both the extrinsic and intrinsic coagulation pathways were activated and played a role in stopping the loss of blood, thus the absence of bleeding at the end of day 0 (Fig. 5a, day 0). This hemostasis marked the onset of the wound healing cascade. By day 7, the inflammatory phase of wound healing had commenced and was characterized by infiltration of the white blood cells and thrombocytes. These cells sped up the inflammatory process by releasing more mediators and cytokines [3, 22]. The presence of valsartan in the scaffolds ensured collagen degradation, transformation of fibroblasts, growth of new vessels, and commencement of re-epithelialization [22]. Figure 5c showed the comparative size reduction of the wounds treated with the scaffolds and controls indicating an onset of the proliferation stage of wound healing which occurred from day 8 to day 14. The proliferative or granulation phase does not occur

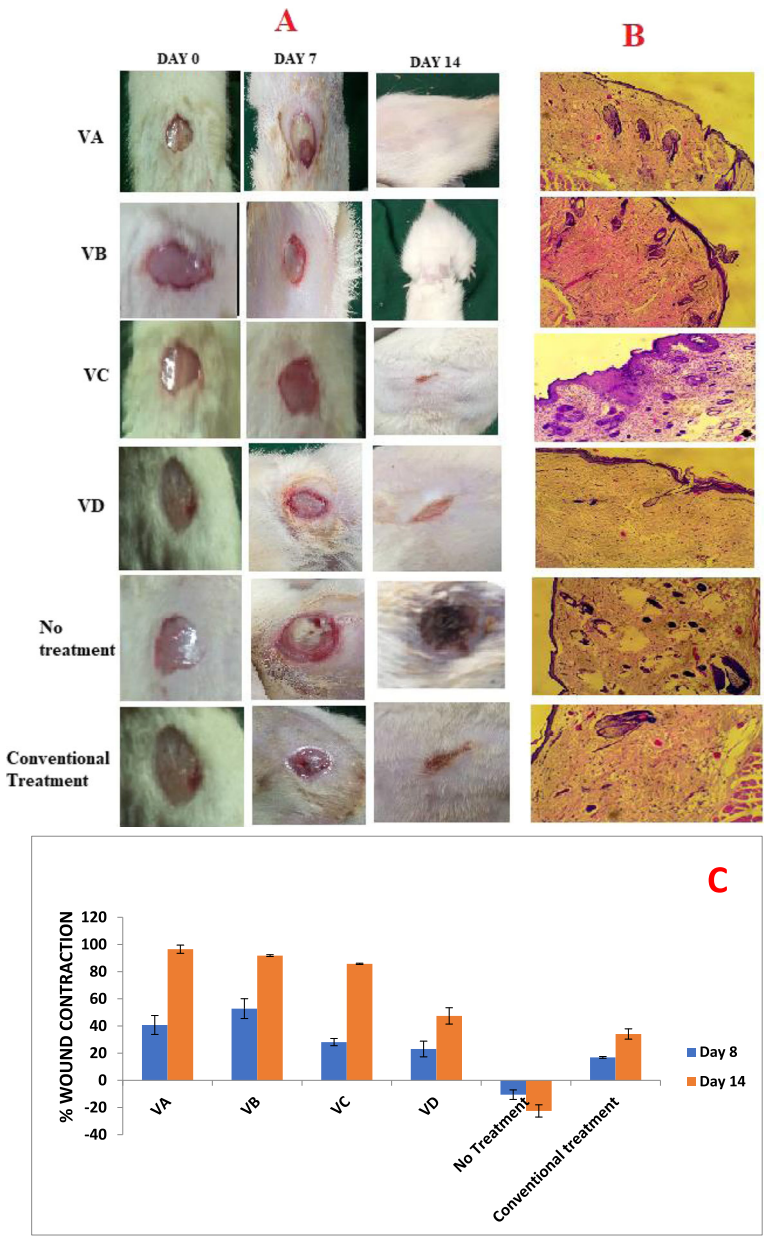

Fig. 5 a Representative images of wounds as days elapsed showing marked difference between varying PLA/HA-valsartan scaffolds VA, VB, VC, and VC, no treatment group cover with gauze and conventional treatment Sofratulle gauze containing fraymycetin sulfate BP 1%. **b** Representative sections stained with hematoxylin and eosin 15 days post-treatment (H&E). **c** Percentage wound contraction in the animals treated with varying PLA/HA-valsartan scaffolds and control. *N* = 4

at a discrete time but concurrently with wound bed maturation [7]. By days 6 to 8, the animals experienced an initiation of collagen out lay via fibroblast activity; this was evidenced by the percentage occupied by collagen in granulation tissue (%/mm^2 of field) (Fig. 6d) which was measured by day 14. Re-epithelialization starts to occur with the migration of cells from the wound periphery and adjacent edges. Initially, only a thin superficial layer of epithelial cells is laid down, but with time, a thicker and more durable layer of cells was seen to act as a bridge across the wound bed and this was seen on days 7–9. In the animals treated with VA and VB, maturation and re-modeling phase occurred by day 13. Neovascularization which is the formation of new blood vessels from existing vessels was still occurring by day 13 in animals treated with VC, VD, and control hence the presence of open wound and reduced wound bed closure as shown in Fig. 5, day 14. The onset of both proliferation and modeling phase varied in all the study animals depending on the treatment protocol applied. Maturation was evident with complete wound

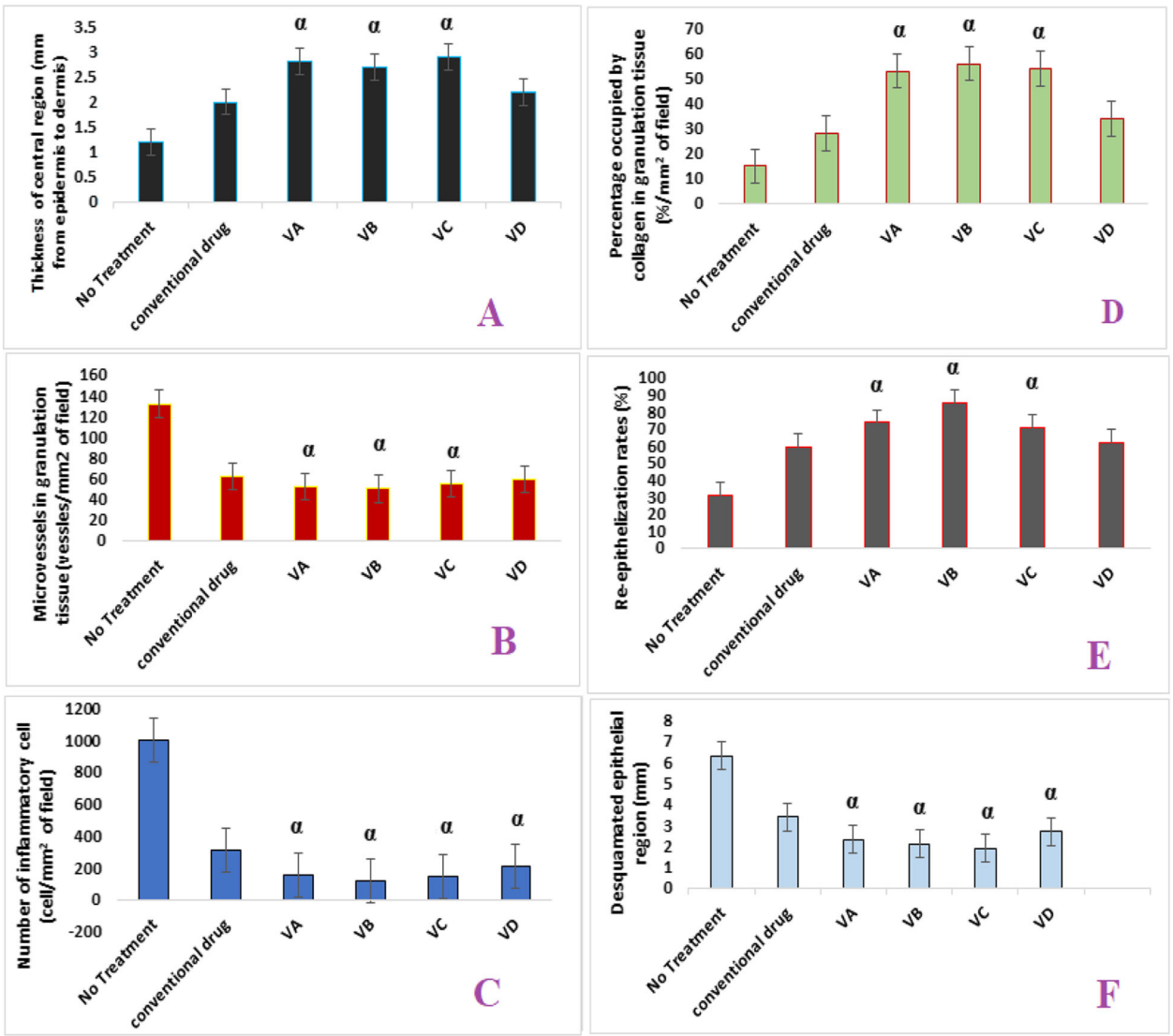

Fig. 6 Histomorphometrical values showing **a** thickness of central region (mm from epidermis to dermis), **b** microvessels in granulation tissue (vessels/mm^2 of field), **c** number of inflammatory cells (cell/mm^2 of field), **d** percentage occupied by collagen in granulation tissue (%/mm^2 of field), **e** re-epithelization rates (%), and **f** desquamated epithelial region (mm). Treatments were compared with control (conventional drug Sofratulle® containing 1% framycetin sulfate) (α reflects significance, $^{\alpha}p < 0.05$. $n = 4$). The composition of PLA/HA-valsartan scaffolds VA, VB, VC, and VD is provided in Table 1

contraction and skin remodeling by day 14 in animals treated with VA and VB (Fig. 5a). The rats in the no-treatment group did not exhibit the proliferation and maturation stage of wound healing. The normal wound healing process was disrupted via induction of diabetes, and the presence of necrosis was observed in Fig. 5a, day 14 for this group.

The scaffolds considerably reduced the wound size in comparison with the antiseptic gauze, as the difference in the healed areas between the different hydrogel-loaded nanofiber samples and the sterile gauze was statistically significant. Histologic section of tissue shows skin with underlying loose fibro collagenous stroma (dermis) containing sebaceous glands and hair follicles for VA, VB, VC, and VD. No abnormalities were seen in the sections for VA, VB, VC, and VD (Fig. 5b). However, in the conventional treatment, there was an increased number of inflammatory cells observed in both control (without treatment) and with conventional treatment (Fig. 6c). Histomorphometrical values showed a statistically significant difference in the healing response of the animals, i.e., a variation for the onset of proliferation, maturation/remodeling phase of the wound healing cascade. The concentration of valsartan incorporated into the formulation was not a determinant of the rate of wound closure. The presence of valsartan significantly

impacted on the re-epithelization rate. Percentage re-epithelization rate was 31.2% ± 1.77% in the absence of treatment (Fig. 6e). The dermis of all the subject animals was infiltrated by dense aggregates of inflammatory red cells (Figs. 5b and 6c). However, all the scaffolds irrespective of whether they contained valsartan or not reduced the number of inflammatory cell infiltrates at the wound site compared to the no treatment and conventionally treated groups. Conventional antibiotic treatment and VD (electrospun biomimetic scaffolds containing ascorbic acid) had % re-epithelization rates of 59.45% ± 1.69% and 62.01% ± 1.68% which were significantly lower than the PLA/HA-valsartan hydrogel scaffolds with VB having the highest % re-epithelization rate of 85.5% ± 1.7% (Figs. 5b and 6c)

4 Discussion

Hydrogels have shown promise as wound dressing materials as they are able to create a hydrated environment to help promote the body's wound healing response [12, 16, 24]. This research studied the development and characterization of PLA-based electrospun nanofibers loaded with hyaluronic acid hydrogel containing valsartan and ascorbic acid for chronic wound healing. The use of nanofibers has gained importance in wound healing in the health industry due to its ability to mimic the human extracellular matrix. Nanofibers can deliver various agents to local tissues at the wound site, like drugs, herbal extracts [5], and growth factors, i.e., EGF (epidermal growth factor) [4]. Electrospun matrices also have a large specific surface area-to-volume ratio, high porosity, and ease of control over the diameter, composition, and morphology of the constituent fibers [11]. The renin-angiotensin system is involved in the inflammatory response, collagen deposition, and transforming growth factor-beta (TGFβ) signaling necessary for wound healing [25]; hence, this study seeks to explore the use of biomimetic electrospun fibers incorporating a topical angiotensin receptor blocker to accelerate wound healing. Chronic wounds exhibit a pH around 7.15–8.90 at the wound bed, creating a slightly basic environment [26]. Metalloproteinase enzymes degrade proteins more rapidly in basic conditions, consuming more oxygen from the tissue to speed up the process. Therefore, the hyaluronic acid hydrogel formulated with an acidic pH when incorporated into the PLA backbone has the potential to slow metalloproteinase enzyme degradation rates hence decreasing abnormal collagen in the wound bed. This will increase fibroblast activity and enhance the toxicity of the environment to bacteria, thus enabling effective wound healing. This was acutely observed in the electrospun fiber VD, which did not contain valsartan but still actively increased re-epithelization rate (Fig. 6e) and reduced the number of micro-vessels in the granulation tissue of the diabetic rats utilized in this study (Fig. 6b) [26]. The effective use of valsartan containing hydrogel in animal models in the treatment of chronic diabetic wounds has also been demonstrated to aid angiogenesis, increased fibroblast proliferation, re-epithelization, reduced oxidative stress, and increased blood flow to the site of injury [6].

The small fiber diameters inherent in the fabricated electrospun fibers offer large surface area-to-volume ratio resulting in high porosity, enhanced drug solubility, and versatile surface functionalization, unlike conventional sterile gauze dressings that have a diameter of 25–100 mm [7]. Wound healing dressings possessing small fiber diameters also ensure protection against bacterial contaminants hence the reason why VD, which did not contain either valsartan or an antibiotic agent, was able to have comparable wound healing activity with the conventional wound dressing. The presence of PLA as the nanofiber backbone which was loaded with hydrogel matrix containing an antioxidant provided an excellent biomimetic matrix for wound healing. The high porosity of the scaffolds VA–VD ensured excellent oxygen permeability, which is essential to generate energy for the wound healing process including matrix synthesis, cell migration, and proliferation while also promoting body fluid absorption and diffusion of waste [27].

The tensile strength and elastic modulus of the human skin has been recorded as 1–32 MPa and 15–150 MPa respectively [28]. This suggests that the mechanical properties of the formulation can closely match the mechanical properties of the human skin. This also suggests that there is effective attachment of the compounds in the hydrogels and the PLA chains. The melting temperature (Tm) of sample VA, VB, VC, and VD at 171.61, 158.10, 156.57, and 133.06 °C, respectively, also showed a slight variation from normal values for PLA (173–178 °C) [22]. Differences in these values may be due to the difference in concentrations of hydrogels loaded into the fibers. Comparisons between VA, VB, and VC showed that there was no statistically significant difference between the cumulative release of valsartan from VA and VC and that there is a statistically significant difference in the cumulative release of valsartan from VB compared to VA and VC. However, VB showed a higher cumulative release of valsartan from the hydrogel scaffolds than VA and VC. The results suggest that valsartan release from the scaffolds is controlled. This thus offers numerous advantages, like maintenance of an optimum drug concentration and increased duration of therapeutic effect. The formulations containing valsartan (VA, VB, and VC) also showed better wound closure than VD which did not contain valsartan. Valsartan-mediated wound healing was seen to accelerate healing rate via increased wound blood flow, collagen deposition, and re-epithelialization hence increase remodeling which led to increased tensile strength of healing skin. These results are consistent with prior reports on the

effects of the RAS on skeletal muscle repair and demonstrate the efficacy of topical ARBs in chronic wound healing [6]. The hydrogel-loaded nanofiber scaffolds promoted growth and migration of healthy cells in wound bed of the diabetic rats. Bioactive wound dressings have the ability to excessively absorb water at the wound bed, thus providing a suitable environment for bacterial growth [5, 7, 9]. However, our results indicated that this was an unjustified concern as the hydrogel scaffolds were able to inhibit bacterial growth and proliferation due to the presence of acid groups in their structure and creation of an environment with an appropriate pH. Histological analysis was conducted to investigate the diabetic wound healing activity of the formulations more specifically. Faghih et al. [29] showed that there was a significant increase in angiotensin type 1 receptors and tissue-related growth factor β1 and β2 expression during the proliferative and remodeling phases in angiotensin type 1 receptor mice. Despite the accelerated closure rate, angiotensin type 1 receptor mice had more fragile healed skin. This is not in consonance with studies by Abadir et al. [6] who postulated that utilization of valsartan 1% gel had the ability to regenerate collagen in aged skin suggesting age-related skin fragility may be reversed and may prove useful in other diseases. This result is in consonance with the present study where the histopathological images of the treated rat skin revealed a continuous and thick epithelial layer with underlying loose fibro-collagenous stroma (dermis). The epithelial layer contained sebaceous glands and hair follicles in all groups, with VA, VB, and VC showing a complete epithelization and good collagen deposition. The group treated with VC however showed a thin epithelial layer due to the absence of valsartan from this scaffold. Dense aggregates of inflammatory red cells can also be seen in the groups treated with the conventional treatment. This heightened inflammatory phase characterized by abundant neutrophil infiltration to the site of injury could explain the slower wound contraction rate observed in the groups treated with the conventional treatment, compared to the groups treated with the hydrogel scaffolds. A short wound closure time may not necessarily coincide with complete maturation and wound remodeling [29–32]. The activity of polylactic acid-based electrospun fiber and HA-valsartan hydrogel scaffold on the quality of wound repair was most significant in the scaffolds containing valsartan. Wound healing was greatly accelerated with the presence of valsartan in the scaffolds with the thickness of the central region of the epidermis to the dermis being the highest in the PLA/HA-valsartan treated scaffolds (VB 2.8 mm ± 0.02 vs. no treatment 1.2 mm ± 0.04 and conventional treatment of 1% framycetin 2 mm ± 0.01 $^{\alpha}P < 0.05$). HA-valsartan hydrogel scaffold treatment yielded significantly stronger healing skin with visible hair regrowth suggestive of a deterrent against wound dehiscence which is critical in diabetic wound care. Our research demonstrates that the PLA/HA-valsartan-treated scaffold VB increased the rate of a chronic wound healing in diabetic rats. The accelerated healing rate was associated with increased wound blood flow due to the presence of valsartan, increased percentage occupied by collagen in granulation tissue, and increased re-epithelialization and led to a full wound closure which is consistent with the results from pig models of Rodgers et al. [33], which demonstrated increased collagen deposition with topical valsartan treatment. The PLA/HA-valsartan-treated scaffold VB which enhanced collagen deposition may be applied as a novel treatment management option for the use of topical ARBs in skin wrinkling and maxillofacial reconstructive surgery.

5 Conclusion

This study explored the used of biomimetic polylactic acid-based electrospun fiber and HA-valsartan hydrogel scaffold incorporating a topical angiotensin receptor blocker to successfully accelerate wound healing. PLA-based electrospun fibers loaded with hyaluronic acid hydrogel containing valsartan were stable and possessed diabetic wound healing property. This was as a result of the known biomimetic effect of the fibers and increased re-epithelization facilitated by the hydrogels containing valsartan. The controlled release of valsartan from the scaffold VB facilitated improved blood flow to the wound site hence ensuring complete remodeling of the wound area.

Abbreviations

PLA: Polylactic acid; PLA/HA: Polylactic acid/hyaluronic acid; MRSA: Methicillin-resistant staphylococcus aureus; SEM: Scanning electron microscopy; DSC: Differential scanning calorimetry; PBS: Phosphate-buffered saline

Acknowledgements

The content is solely the responsibility of the authors.
The authors acknowledge the technical effort of Mr Olaleye from the Department of Metallurgical and Materials Engineering, Faculty of Engineering, University ofLagos during the electrospinning procedure.

Authors' contributions

MOI conceived the study. MOI, JNA, and SOA helped design and coordinate the study. PSO, JCO, OOO, and BOS carried out the experimental studies. MOI and OOO drafted the manuscript. All authors have read and approved the final manuscript.

Funding

Not applicable.

Availability of data and materials

Data is contained in the manuscript.

Ethics approval and consent to participate

Ethical approval was obtained from the Health Research and Ethics Committee of the College of Medicine University of Lagos. All the experiments accorded with the Institution Guidelines and were approved by

the College of Medicine University of Lagos Health Research Ethical Committee CMUL/HREC/07/19/564.

Consent for publication
Not applicable.

Competing interests
The authors declare that they have no competing interests.

Author details
[1]Department of Pharmaceutics and Pharmaceutical Technology, Faculty of Pharmacy, University of Lagos, PMB 12003, Surulere, Lagos, Nigeria. [2]Center for Biomedical Research, Population Council, 1200 York Avenue, New York 10065, USA. [3]Department of Metallurgical and Materials Engineering, Faculty of Engineering, University of Lagos, PMB 12003, Surulere, Lagos, Nigeria.

Received: 28 February 2020 Accepted: 20 May 2020
Published online: 10 August 2020

References
1. Leaper D (2006) Silver dressings: their role in wound management. *Int Wound J* 3:282–294 https://doi.org/10.1111/j.1742-481X.2006.00265.x
2. Rushton I (2007) Understanding the role of proteases and pH in wound healing. *Nurs Stand* 21:68–72 https://doi.org/10.7748/ns2007.04.21.32.68.c4499
3. Bonvallet P, Matthew J, Elizabeth H, Bain J, Culpepper B, Thomas S, Bellis S (2015) Microporous dermal-mimetic electrospun scaffolds pre-seeded with fibroblasts promote tissue generation in full-thickness skin wounds. *PLoS One* 10:1–17 https://doi.org/10.1371/journal.pone.0122359
4. Thakkar S, Misra M (2017) Electrospun polymeric nanofibers: new horizons in drug delivery. *Eur J Pharm Sci* 10:1393–1399 https://doi.org/10.1016/j.ejps.2017.07.001
5. Suganya S, Venugopal J, Agnes Mary S, Ramakrishna S, Lakshmi B, Giri V (2014) Aloe vera incorporated biomimetic nanofibrous scaffold: a regenerative approach for skin tissue engineering. *Iran Polym J* 23:237–248 https://doi.org/10.1007/s13726-013-0219-2
6. Abadir P, Sayed H, Mahya F, Amir A, Frank L, Barbara S, Aleksandra B, Diep V, Alan B, Jing T, David R, Kevin K, Joshua B, Tadashi I, Neal F, Guy M, John H, Walston J (2018) Topical reformulation of valsartan for treatment of chronic diabetic wounds. J Investig Dermatol 138:434–443 https://doi.org/10.1016/j.jid.2017.09.030
7. Ilomuanya MO, Adeyinka O, Aghaizu C, Cardoso-Daodu I, Akhimien T, Ajayi T et al (2019) Co-formulation and characterization of gentamicin-loaded alkyl acrylate cross polymer hydrogel infused with ethanol extract of *Tetracarpidium* conophorum impregnated on gauze sponge for wound dressing. Wound Healing Southern Africa 12(1):22–28 https://journals.co.za/content/journal/10520/EJC-17b07e7ea5
8. Song W, Liang D, Hanson H, Kai X, Yu H, Qiangru H, Yi P, Zhihua Z, Cheng P (2017) Evaluation of gelatin-hyaluronic acid composite hydrogels for accelerating wound healing. *J Biomater Appl* 31(10):1380–1390 https://doi.org/10.1177/0885328217702526
9. Gilmartin D, Alexaline M, Thrasivoulou C, Phillips A, Jayasinghe S, Becker D (2013) Integration of scaffolds into full thickness wounds: the connexin response. *Adv Healthcare Mater* 2:1151 https://doi.org/10.1002/adhm.201200357
10. Yang Y, Ritchie A, Everitt N (2017) Comparison of glutaraldehyde and procyanidin cross-linked scaffolds for soft tissue engineering. *Mater Sci Eng* 80:263–273 https://doi.org/10.1016/j.msec.2017.05.141
11. Jayarama V, Radhakrishnan S, Ravichandran R, Mukherjee S, Balamurugan R, Sundarrajan S, Ramakrishna S (2013) Nanofibrous structured biomimetic strategies for skin tissue regeneration. *Wound Repair Regen* 21(1):1–16 https://doi.org/10.1111/j.1524-475X.2012.00861.x
12. Kamoun E, Kenawy E, Chen X (2017) A review on polymeric hydrogel membranes for wound dressing applications: PVA-based hydrogel dressings. *J Adv Res* 8:217–233 https://doi.org/10.1016/j.jare.2017.01.005
13. Barrett D, Hartshorne M, Hussain M, Shaw P, Davies M (2001) Resistance to nonspecific protein adsorption by poly(vinyl alcohol) thin films adsorbed to a poly(styrene) support matrix studied using surface plasmon resonance. *Anal Chem* 73:5–9 https://doi.org/10.1021/ac010368u
14. Zhu J, Li F, Wang X, Yu J, Wu D (2018) Hyaluronic acid and polyethylene glycol hybrid hydrogel encapsulating nanogel with hemostasis and sustainable antibacterial property for wound healing. *ACS Appl Mater Interfaces* 10:13304–13316 https://doi.org/10.1021/acsami.7b18927
15. Bahman E, Mirsepehr P, Ashrafalsadat H, Soheila S, Mahtab R, Zahra BM, Mohammad M (2016) In vivo evaluation of gelatin/hyaluronic acid nanofiber as burn-wound healing and its comparison with ChitoHeal gel. *Fibers and Polymers* 17(6):820–826 https://doi.org/10.1007/s12221-016-6259-4
16. Ilomuanya MO (2020) Chapter 23: Hydrogels as biodegradable biopolymer formulations; Biopolymer-Based Formulations pp: 561-585, ISBN 9780128168974 https://doi.org/10.1016/B978-0-12-816897-4.00023-0, (http://www.sciencedirect.com/science/article/pii/B9780128168974000230)
17. Daulat K, Sajid B, Figueiredob P, Hélder S, Muhammad K, Leena P (2019) Process optimization of ecological probe sonication technique for production of rifampicin loaded niosomes. *Journal of Drug Delivery Science and Technology* 50:27–33 https://doi.org/10.1016/j.jddst.2019.01.012
18. Croisier F, Duwez A, Jerome C, Leonard A, van der Werf K, Dijkstra P, Bennink M (2012) Mechanical testing of electrospun PCL fibers. *Acta Biomater* 8(1):218–224 https://doi.org/10.1016/j.actbio.2011.08.015
19. National Institutes of Health guide for the care and use of laboratory animals (NIH Publication No. 8023, revised in 1978) https://grants.nih.gov/grants/olaw/guide-for-the-care-and-use-of-laboratory-animals.pdf
20. Mendes JJ, Leandro CI, Bonaparte DP, Pinto AL. (2012) A rat model of diabetic wound infection for the evaluation of topical antimicrobial therapies. Comp Med. 62(1):37-48. PMID: 22330650; PMCID: PMC3276391.
21. Brown MS, Ashley B, Koh A (2018) Wearable technology for chronic wound monitoring: current dressings, advancements, and future prospects. *Front Bioeng Biotechnol* 6:47 https://doi.org/10.3389/fbioe.2018.00047
22. Luo W, Cheng L, Yuan C, Wu Z, Yuan G, Hou M, Chen JY, Luo C, Li W (2019) Preparation, characterization and evaluation of cellulose nanocrystal/poly(lactic acid) in situ nanocomposite scaffolds for tissue engineering. Int J Biol Macromol 134:469–479 https://doi.org/10.1016/j.ijbiomac.2019.05.052
23. Gouda R, Himankar B, Zhao Q (2017) Application of mathematical models in drug release kinetics of carbidopa and levodopa ER tablets. *J Develop Drugs* 6:171 https://doi.org/10.4172/2329-6631.1000171
24. Ilomuanya M, Amenaghawon NA, Odimegwu J, Okubanjo OO, Aghaizu C, Adeyinka O, Akhimien T, Ajayi T (2018) Formulation and optimization of gentamicin hydrogel infused with *Tetracarpidium conophorum* extract via a central composite design for topical delivery. Turk J Pharm Sci 15(3):319–327 https://doi.org/10.4274/tjps.33042
25. Hao S, Ren M, Yang C, Lin D, Chen L, Zhu P (2011) Activation of skin renin-angiotensin system in diabetic rats. *Endocrine*. 39:242–250 https://doi.org/10.1007/s12020-010-9428-z
26. Gethin G (2007) The significance of surface pH in chronic wounds. Wounds UK, 2007, Vol 3, No 3 :1-4
27. Hitomi S, Shigeru I, Naomi S (2012) Influence of oxygen on wound healing dynamics: assessment in a novel wound mouse model under a variable oxygen environment. *PLoS One* 7(11):502–512 https://doi.org/10.1371/journal.pone.0050212
28. Shixuan C, Bing L, Mark C, Adrian G, Debra R, Jingwei X (2017) Recent advances in electrospun nanofibers for wound healing. *Nanomedicine*. 12(11):1335–1352 https://doi.org/10.2217/nnm-2017-0017
29. Faghih M, Hosseini SM, Smith B, Ansari AM, Lay F, Ahmed AK, Inagami T, Marti GP, Harmon JW, Walston JD, Abadir PM (2015) Knockout of angiotensin AT2 receptors accelerates healing but impairs quality. Aging (Albany NY) 7(12):1185–1197 https://doi.org/10.18632/aging.100868
30. Hsiao M, Lin A, Liao WH, Wang TG, Hsu CH, Chen WS, Lin FH (2019) Drug-loaded hyaluronic acid hydrogel as a sustained-release regimen with dual effects in early intervention of tendinopathy. *Sci Rep* 9:4784 https://doi.org/10.1038/s41598-019-41410-y
31. Vatankhah E, Prabhakaran MP, Jin G, Mobarakeh LG, Ramakrishna S (2014) Development of nanofibrous cellulose acetate/gelatin skin substitutes for variety wound treatment applications. J Biomater Appl 28(6):909–921
32. Ilomuanya MO, Adebona AC, Wang W, Sowemimo AA, Eziegbo C, Silva BO, Adeosun SO, Joubert E, De Beer D (2020) Development and characterization of collagen-based electrospun scaffolds containing silver sulphadiazine and *Aspalathus linearis* extract for potential wound healing applications. SN Applied Sciences 2:881 https://doi.org/10.1007/s42452-020-2701-8
33. Rodgers K, Verco S, Bolton L, Dizerega G (2011) Accelerated healing of diabetic wounds by NorLeu(3)-angiotensin (1-7). Expert Opin Investig Drugs 20(11):1575–1581 https://doi.org/10.1517/13543784.2011.619976

Publisher's Note